NASA Technical Memorandum 103171

Thermomechanical Testing Techniques for High-Temperature Composites: TMF Behavior of SiC(SCS-6)/Ti-15-3

Michael G. Castelli
Sverdrup Technology, Inc.
Lewis Research Center Group
Brook Park, Ohio

and

J. Rodney Ellis and Paul A. Bartolotta
National Aeronautics and Space Administration
Lewis Research Center
Cleveland, Ohio

Prepared for the
10th Symposium on Composite Materials: Testing and Design
sponsored by the American Society for Testing and Materials
San Francisco, California, April 24-25, 1990

NASA

THERMOMECHANICAL TESTING TECHNIQUES FOR HIGH TEMPERATURE COMPOSITES: TMF BEHAVIOR OF SiC(SCS-6)/Ti-15-3

Michael G. Castelli
Sverdrup Technology, Inc.
Lewis Research Center Group
Brook Park, Ohio 44142

and

J. Rodney Ellis and Paul A. Bartolotta
National Aeronautics and Space Administration
Lewis Research Center
Cleveland, Ohio 44135

ABSTRACT

Thermomechanical testing techniques recently developed for monolithic structural alloys were successfully extended to continuous fiber reinforced composite materials in plate form. The success of this adaptation was verified on a model metal matrix composite (MMC) material, namely SiC(SCS-6)/Ti-15V-3Cr-3Al-3Sn. Effects of heating system type and specimen preparation are also addressed. Cyclic lives determined under full thermomechanical conditions were shown to be significantly reduced from those obtained under comparable isothermal and in-phase bi-thermal conditions. Fractography and metallography from specimens subjected to isothermal, out-of-phase and in-phase conditions reveal distinct differences in damage/failure modes. Isothermal metallography revealed extensive matrix cracking associated with fiber damage throughout the entire cross-section of the specimen. Out-of-phase metallography revealed extensive matrix damage associated with minimal (if any) fiber cracking. However, the damage was located exclusively at surface and near-surface locations. In-phase conditions produced extensive fiber cracking throughout the entire cross-section, associated with minimal (if any) matrix damage.

INTRODUCTION

Metal Matrix and Intermetallic Matrix Composites (MMC and IMC) are being developed for a number of high-temperature aerospace applications. The advantage of these composite materials is that they offer superior strength/density ratios compared to monolithic materials, particularly at elevated temperatures. This level of performance typically is achieved by using high strength ceramic fibers and low density matrix materials. One obvious problem with this approach is that it combines materials with widely differing physical properties. This mismatch raises questions regarding the performance of MMC and IMC materials under the complex thermomechanical loading conditions typical of aerospace service.

The development of reliable thermomechanical testing techniques for this class of materials was viewed as being a logical first step in addressing this concern. The approach adopted was to extend advanced testing techniques recently developed for monolithic structural alloys (ref. 1) such as Hastelloy Alloy-X and Haynes 188 to composite materials in thin plate form. This effort included the development of computer test control software, an advanced heating fixture, a proper specimen design and innovative experimental techniques. To verify the success of this adaptation, the full thermomechanical fatigue (TMF) behavior of a high-temperature composite was investigated.

Specialized real-time control software was developed to perform thermomechanical tests under load, strain and combined load-strain control. One difficulty encountered with thermomechanical testing involves the task of ensuring precise phasing between the controlled variable, load or mechanical strain, and specimen temperature. This problem arises because of the response-time difference which typically exists between the temperature and the mechanical component of loading. Tests performed under conditions of improper phasing will often produce distorted hysteresis loops, making subsequent data reduction and analysis difficult, if not impossible. The approach taken here was to incorporate subtle shifts in the temperature-command waveform at appropriate points in the cycle (i.e., reversals). For example, the temperature-command is reversed prematurely such that the actual temperature response will reverse simultaneously with the mechanical load. Through this

"shifting" of the temperature-command waveform, the temperature-response can be tailored and phased correctly with the mechanical component of loadng.

Another difficulty encountered with uniaxial thermomechanical testing arises under strain control conditions. Under this control mode, thermal strains have a first order effect on the mechanical loading component, namely, the axial strains. In order to properly control the mechanical strains, an accurate assessment of the thermal strains must be made at all times. This task is further complicated if phasing problems exist. The computer code extended for this study incorporates a function to calculate the real-time thermal strains based on a continuous analog-to-digital reading of the specimen's temperature. These calculated thermal strains are then appropriately added to the desired mechanical strains to obtain a total command strain. By this means, a nonlinear thermal expansion can be accurately compensated for to maintain the desired mechanical strain waveform.

Other important issues and problems which must be addressed include minimizing dynamic thermal gradients, temperature monitoring and heating/cooling rates. Procedures were developed to optimize these interrelated variables with respect to specific equipment and test material. Adopting this approach, techniques originally developed for testing monolithic alloys have been successfully extended to composite materials.

OBJECTIVE AND APPROACH

The main objective of this work was to evaluate the extended thermomechanical testing techniques on a model MMC. A silicon carbide continuous fiber reinforced titanium MMC designated SiC(SCS-6)/Ti-15V-3Cr-3Al-3Sn (Ti-15-3) was chosen as the material to be investigated. This particular system was selected because of availability, established processing parameters and well defined mechanical properties. Although the system is not typically thought of as a high temperature material, it is useful as a "characteristic" material for developing and refining high temperature testing techniques.

A second objective was to characterize the TMF behavior of SiC(SCS-6)/Ti-15-3. Recently, the room temperature (refs. 2 and 3), isothermal (ref. 4) and bi-thermal (ref. 5) behavior of this composite system has been investigated. Also, work was performed by Majumdar et al., (ref. 6) to characterize the full TMF behavior of angle-ply laminates. However, very little (if any) information is available addressing the full TMF behavior of the unidirectional system. Lastly, there is some concern in the testing community about the effects of induction heating, and method of specimen preparation on the fatigue life of the test specimens. These issues will be briefly addressed through the comparison of several isothermal fatigue tests.

All material tested here is 9 ply laminate with 0° (longitudinal) fiber orientation. All test specimens had a nominal fiber volume ratio of 34 percent and a nominal thickness of 2 mm. The test specimens were cut from one 30.5 by 30.5 cm plate using wire electric discharge machining (EDM), followed by a light diamond grinding. Although the Ti-15-3 matrix material is a stabilized beta (bcc) phase, long term exposures at elevated temperatures can lead to the precipitation of a α-Ti phase (refs. 7 to 9). This primary hardening phase has been shown by several investigators to affect the mechanical properties. Therefore, to stabilize the material, the specimens were heat treated in a vacuum at 700 °C for a 24 hr period.[1]

The specimen geometry used for this investigation is shown in figure 1. The "dogbone" design features a 25.4 mm parallel section to facilitate close control of the temperature profile. Tabs were attached to the specimen with adhesive for assembly purposes, and held in position by high clamping forces during the test.

All TMF experiments were conducted on a computer controlled, servo-hydraulic test system; a close-up of the load train is shown in figure 2. Specimen heating was accomplished through direct induction work coils powered by a 5 kW radio-frequency heater. The induction coil fixture used here consists of three independently adjustable coil segments. This fixture, developed at NASA Lewis Research Center (ref. 10), provided the flexibility necessary to obtain closely controlled dynamic temperature profiles. Specimen cooling was accomplished through the combination of water-

[1]Although the heat treatment improved the microstructural stability, it is believed that the material was still slightly metastable.

cooled grips and forced air. Although forced air creates difficulties when attempting to attain very precise temperature profiles, it was necessary here to obtain a target cycle period of 3 min. Intrinsic (spot-welded) K-type thermocouples were used for temperature monitoring and closed-loop control. The thermocouple locations did not exhibit premature cracking, and hence had no influence on the fatigue life of the specimen. Axial strains were measured over a 12.7 mm gauge section on the edge of the specimen by a high temperature water-cooled extensometer. A selected number of baseline isothermal experiments were also conducted to investigate the effects of heating system type and method of specimen preparation. For these tests, a small two-zone direct resistance furnace was used to heat the specimens.

The test matrix performed for this study is given in figure 3. All tests were run under load control. The isothermal tests were conducted at 427 °C, where a triangular load control function was cycled with a frequency of 10 cycles/min. As a result of the specimen's geometry, compressive loads would induce buckling, therefore, all tests (including thermomechanical) were run to failure under cyclic tension-tension conditions with a minimum/maximum stress ratio, (R_σ), of 0.05. The TMF tests were conducted with both sinusoidal load and temperature control waveforms. Both in-phase and out-of-phase (180° phase shift between maximum load and maximum temperature) conditions were run with a cycle period of 3 min, and a temperature range of 93 to 538 °C.

As mentioned above, thermomechanical conditions introduce several new concerns associated with high temperature testing. Previous testing performed on monolithic alloys (ref. 1) revealed that the dynamic thermal gradients were significantly greater than the static gradients existing before temperature cycling was initiated. Further, the dynamic gradient at any one location did not remain constant throughout the cycle, rather, it was found to cyclically fluctuate with the temperature magnitude. The degree of these effects were found to depend upon variables such as temperature range, temperature magnitude and cycle period. The approach taken to minimize dynamic thermal gradients involves establishing an appropriately imposed isothermal/static gradient at some midcycle temperature. This technique is given in detail in (ref. 1). Shown in figure 4 is a typical dynamic temperature profile (longitudinal) taken from a TMF experiment. Note the variable dynamic gradient, illustrated by the changing distances between the respective curves. The three most closely grouped curves represent the gradients within the gauge section, which experienced a maximum (≈15 °C) at the "hot" end of the cycle. This value was typical for all of the TMF tests.

The TMF test specimens were thermally cycled under zero load prior to mechanical loading in order to quantify the thermal strains and ensure that a stable strain response existed. This cycling did not exceed 10 cycles because the temperature-strain response was found to be initially stable.

RESULTS AND DISCUSSION

Isothermal fatigue results are plotted as life curves on a stress basis in figure 5. Also shown in this plot are duplicate tests generated by Ervin et al., (Pratt and Whitney) and similar tests generated by Gayda et al., (NASA Lewis) (unpublished data obtained through personal communication). The same material and specimen geometry was used for all the tests. In each case, failure is defined as complete fracture of the specimen into two pieces. The three sets of data compared were generated employing a combination of specimen preparation and specimen heating methods. For specimen preparation, Gayda et al., utilized wire EDM cutting followed by light diamond grinding, whereas Ervin et al., employed water jet cutting followed by hand polishing. For specimen heating, Gayda et al., utilized direct induction and Ervin et al., employed radiant heating. As shown in figure 5, the various cyclic fatigue lives are in very good agreement. This result was particularly surprising, given that the data were generated by three independent experimental groups.

An initial interpretation may be that the isothermal cyclic fatigue lives of this unidirectional composite material are not sensitive to the method of specimen preparation or method of heating. However, it is important to note that there are several issues of concern which need to be addressed, particularly in regard to specimen design. The test specimens are cut from a large, continuously reinforced plate, and as a result, contain cut fibers along the edges. These locations are potential stress concentration/crack initiation points. Also, the specimens are tested with "as-received" surface conditions which, from the traditional fatigue viewpoint, were less than ideal. Further, the majority of as-manufactured specimens exhibited curvature along their length, introduced into the original 30.5 by 30.5 cm plate during processing. Clearly, this curvature leads to nonuniform stress-strain states being developed in the specimens upon gripping and loading. Another area of concern is that the majority of the specimens failed at the blend between the parallel section and the beginning of the radius. Given these uncertainties, another interpretation of figure 5 may be

that one or all of these effects play an important role in dictating the fatigue life of the test specimen. If this were the case, the plot would suggest that the effects promoted by method of specimen preparation and method of heating are secondary issues of concern, at least for the unidirectional material under investigation.

The stress-strain response for two of the isothermal tests is given in figure 6. Shown are the first and second cycle, and a cycle close to failure for tests performed with maximum stresses of 896 and 1034 MPa. The strain offset between these cycles is that which naturally accumulated throughout the test. The cyclic strain ranges were found to change very little throughout the tests, suggesting minimal modulus degradation. However, as shown in figure 7, the cyclic mean strains significantly increased over the first several thousand cycles and continued to increase gradually throughout the life of the specimens. This ratchetting effect was amplified as stress range was increased.

Typical Scanning Electron Microscope (SEM) fractographs taken from the σ_{max} = 896 MPa isothermal specimen are shown in figure 8. In general, the fracture surfaces from all of the isothermal specimens were very similar, revealing flat regions of fatigue cracking accompanied by randomly distributed areas of fiber pull-out and ductile matrix failure. The higher stressed specimens displayed a slightly increased amount of fiber pull-out and ductile matrix failure. Oxidation patterns and SEM backscatter imagery strongly suggest that matrix cracking was initiated at both surface and internal fiber/matrix interface locations. Matrix "river" patterns suggest that there were numerous crack initiation points, and that the cracks have propagated only short distances ($\approx$1 to 2 fiber rows) before coalescing. This relatively short crack growth may be a result of the fibers hindering fatigue crack growth.

Results from the TMF tests are plotted in figure 9 as life curves on a stress basis. For reference purposes, the isothermal fatigue line displayed in figure 5 is also shown in this figure. In general, cyclic lives determined under full TMF conditions were greatly reduced from those obtained under comparable isothermal conditions. Also, for the case of high stress in-phase loadings, lives were reduced by several orders of magnitude from those obtained under comparable isothermal and bi-thermal (nonisothermal) conditions. This magnitude of degradation is best illustrated in figure 9 by a line drawn through σ_{max} = 1034 MPa. The 538 °C isothermal datum point was obtained from a specimen subjected to fatigue cycling with a 3 min cycle period. This condition was imposed to address the effects (i.e., increased ratchetting, environmental) of the relatively slow cycle period. The isothermal specimen experienced a fatigue life of approximately 4000 cycles, whereas the specimens subjected to true in-phase loading conditions from 93° to 538 °C consistently failed upon the second load-up.

The large magnitude of life degradation resulting from true in-phase conditions was not seen under in-phase bi-thermal (nonisothermal) conditions (ref. 6) where a 3 to 4X decrease from isothermal life was obtained. The decreased life displayed under full TMF conditions may be attributed to factors (not present under bi-thermal conditions) promoting minimized reversed inelastic strains in the matrix and thus increased ratchetting (discussed later). One obvious condition promoting damage is that attributed to the coefficient of thermal expansion (CTE) mismatch. Work performed by Gabb et al., (ref. 6) on this MMC system revealed that specimens subjected to 10 000 thermal cycles (from 300° to 550 °C) under zero load did not exhibit degraded mechanical responses during subsequent tests. However, the CTE mismatch did promote highly localized cracks in the reaction zone and carbon-rich coating of the fibers. True thermomechanical conditions introduce this damaging effect from the CTE mismatch as a dynamic component compounded with the transverse Poisson's effects associated with mechanical loading.

The stress-mechanical strain response for an out-of-phase and in-phase test with σ_{max} = 896 MPa is shown in figure 10. Note that the hysteresis loops do not exhibit irregular distortions. This is an essential check in verifying that the thermomechanical test is well controlled. Again, the first two cycles, and a cycle just before failure is plotted, where the mechanical strain offset is that which naturally occurred throughout the test.

In general, the out-of-phase hysteresis loops (fig. 10(a)) were open, displaying evidence of inelastic deformation in any given cycle. Of the three conditions (isothermal, out-of-phase and in-phase), only the specimens subjected to out-of-phase loadings displayed a noticeable change in compliance. This change in compliance is evidenced by an overall change in slope of the TMF loop. Out-of-phase TMF involves "cold" temperatures at high stress and "hot" temperatures at low stress. This condition is not conducive to creep-ratchetting effects, and thus, as shown in figure 11, the behavior reveals gradual increases in mean strain at the onset of the test. This increase is

followed by a subtle decrease in mean strain, as a possible result of matrix work hardening and/or the precipitation of the α-Ti phase. Also, specimens subjected to out-of-phase conditions displayed substantial increases in mean strain late in life ($N > 0.7N_f$), suggesting failure was approaching.

In-phase thermomechanical cycling involves "hot" temperatures at high stress and "cold" temperatures at low stress. This, combined with the specific test parameters selected for the TMF experiments, results in conditions which are highly conducive to creep-ratchetting. Specifically, several parameters can be identified; (1) high stress coinciding with high temperatures, (2) a load control environment where strain limitations are not imposed, (3) a sinusoidal control waveform which lingers at the function's extremes, (4) a relatively slow cycle period of 3 min and, (5) a tension-tension cycle where reversed inelastic strains are minimal. The ratchetting attributed to minimized reversed inelastic strains is further amplified by an increasing elastic modulus (due to a temperature decrease) during unload. This "cold", "nearly-elastic" unload is absent under in-phase bi-thermal conditions (ref. 6), and hence may contribute to the differences in cyclic fatigue lives discussed earlier.

As shown in figures 10(b) and 12, the in-phase loading response exhibits an extensive increase in mean strain (creep-ratchetting) during the initial cycles. This "unrestrained" ratchetting is believed to be the primary cause of the dramatic decrease in fatigue life when compared with out-of-phase TMF conditions. At 538 °C, the titanium-based matrix will tend to creep readily (ref. 11). At these high temperatures, the matrix is unable to carry its share (on a rule of mixtures basis) of the load, therefore, it will tend to relax as if in a strain controlled environment. The load shed by the matrix is distributed to the fibers, thus causing an increased fiber stress and composite mean strain. This process gradually continues at a decreasing rate (due to hardening of the matrix) until eventual fiber overload occurs. This process occurs under isothermal (ref. 5) and bi-thermal (ref. 6) conditions, but is greatly accelerated under in-phase TMF conditions as a result of the factors leading to minimal reversed inelastic strains. The mean strain response tended to stabilize early in life and did not experience an increase late in life as seen under out-of-phase conditions (compare with fig. 11); thus there was no phenomenological indication that failure was approaching. Also, as evidenced in figure 10(b), there was no detectable change in compliance for specimens subjected to in-phase loadings.

Typical SEM fractographs taken from a specimen subjected to out-of-phase loading conditions, σ_{max} = 896 MPa, are shown in figure 13. The fracture surface reveals a fair amount of fatigue cracking, but in general, the area associated with tensile overload appears to be larger than that found in comparable isothermal specimens. True thermomechanical conditions appear to have introduced crack initiation and propagation mechanisms different from those found under isothermal conditions. Oxidation patterns and SEM imagery clearly suggest that crack initiation sites occurred almost exclusively at surface and near-surface fiber-matrix interface locations. Out-of-phase conditions consistently produce fracture surfaces displaying an outer "ring" of oxidized cracking (approximately 2 to 3 fibers into the cross-section) surrounding an internal region exhibiting ductile matrix failure and fiber pull-out. This suggests that the surface plays a decisive role in the damage processes. Also, matrix "river" patterns reveal that individual cracks are less numerous (compared to isothermal fracture surfaces) and appear to have propagated greater distances, as illustrated upon comparing figures 8 and 13. Under out-of phase conditions, the fibers appear less effective at arresting the crack growth.

Typical longitudinal and transverse sections taken from an out-of-phase specimen (σ_{max} = 896 MPa) are shown in figure 14. The sections reveal that the primary cyclic fatigue damage consists of transverse matrix cracking. This cracking was clearly found to initiate at surface locations and near-surface fiber-matrix interfaces. Very little fiber damage was visible. A matrix dominated failure, initiated by matrix microcracking at these locations, is compatible with the fact that the out-of-phase conditions maximize the longitudinal stresses in the matrix; matrix stresses produced by the mechanical loading and thermal expansion mismatch are additive.

In contrast, metallography from specimens subjected to in-phase TMF conditions exhibits trends which are quite different from those seen in isothermal and out-of-phase TMF specimens. Typical SEM fractographs taken from an in-phase specimen, σ_{max} = 896 MPa, are shown in figure 15. This figure reveals extensive fiber pull-out and ductile matrix failure across the entire fracture surface. In fact, the features illustrated here (and from all other in-phase tests performed) most closely resemble those displayed by specimens subjected to tensile tests (ref. 12). This pattern of

pure tensile overload and lack of matrix cracking was a somewhat surprising result, given that several of the lower stress tests experienced well over 1000 cycles.

Longitudinal, shown in figure 16, and transverse sections taken from the gauge section (away from the fracture surface) clearly reveal extensive fiber damage in the absence of matrix cracking (A scenario which is completely opposite to that displayed by the out-of-phase metallography). Fiber cracking was found in both the transverse (more predominant) and longitudinal directions. The fiber dominated failure found under in-phase conditions is also compatible with the fact that in-phase conditions maximize the longitudinal stresses in the fiber, where fiber stresses produced by mechanical loading and thermal expansion mismatch are additive.

Because the results presented here are influenced by the particular test parameters, it is important to note that dramatically different material behavior and resulting fatigue lives can be produced by changing these test parameters. By changing the control mode from load to strain, several of the prime factors leading to extreme creep-ratchetting during in-phase TMF can be eliminated. A similar argument can be used when considering the use of a triangular control function, rather than the sinusoidal employed here, since the sinusoidal function lingers at the extremes. Further, the advent of computer controlled testing has enabled any combination of mixed-mode and mixed-function control. For example, a load controlled test exhibiting a fixed stress rate can be performed with limiting strain boundaries. The ongoing debate addressing the appropriateness of "load control" or "strain control" will most likely never be resolved. However, "test induced" effects, such as creep-ratchetting, should be an issue of concern, both before the tests are performed and during subsequent data interpretation and analysis.

CONCLUSIONS

Improved thermomechanical testing techniques developed for monolithic materials were successfully extended to SiC/Ti-15-3 in plate form. As a result, closely controlled TMF tests were performed with minimal experimental uncertainties. Isothermal fatigue life data did not reveal any sensitivity to heating method (direct induction versus radiant) or specimen preparation method (water cutting/hand polishing versus wire EDM/light diamond grinding). This was evidenced by the close agreement existing among tests generated by three independent experimental groups. However, several key concerns were identified as potentially having a degrading effect on the cyclic fatigue life of the test specimen. These issues are currently being addressed through the investigation of new specimen geometries which minimize stress concentrations, as well as through techniques which lead to test specimens containing completely encapsulated, uncut fibers.

The isothermal data exhibited an essentially linear response after the first cycle with no evidence of modulus degradation throughout the test, however, significant increases in mean strain developed with the majority of this occurring early in the cyclic life. Metallography revealed a large amount of flat fatigue cracking throughout the cross-section of the specimen.

Cyclic fatigue lives were greatly reduced under TMF conditions when compared to isothermal and in-phase bi-thermal data. This was particularly the case for in-phase loadings at high stresses where lives were decreased by several orders of magnitude.

Failure modes displayed under TMF conditions were significantly different from those displayed under comparable isothermal conditions. Out-of-phase loadings clearly displayed a matrix dominated failure, where cracking and crack initiation points were found exclusively at surface locations and near-surface interface locations. In-phase TMF loadings displayed fiber dominated failures, where extensive fiber damage was found in the absence of matrix cracking.

ACKNOWLEDGMENTS

The authors wish to acknowledge Tim Gabb and Ralph Corner for their work on the SEM and optical microscope, and Ron Shinn for his technical assistance with the servo-hydraulic load frames.

REFERENCES

1. Castelli, M.G., "Thermomechanical Deformation Testing and Modeling in the Presence of Metallurgical Instabilities," NASA Report CR-185188, National Aeronautics and Space Administration, Lewis Research Center, Cleveland, OH, Jan. 1990.

2. Johnson, W.S., Lubowinski, S.J., Highsmith, A.L., Brewer, W.D., and Hoogstraten, C.A., "Mechanical Characterization of SCS_6/Ti-15-3 Metal Matrix Composites at Room Temperature," NASA Report NASP TM-1014, National Aeronautics and Space Administration, Langley Research Center, Hampton, Va, Apr. 1988.

3. Johnson, W.S., "Fatigue Testing and Damage Development in Continuous Fiber Reinforced Metal Matrix Composites," NASA Report TM-100628, National Aeronautics and Space Administration, Langley Research Center, Hampton, VA, June, 1988.

4. Gayda, J.G., Gabb, T.P., and Freed, A.D., "The Isothermal Fatigue Behavior of a Unidirectional SiC/Ti Composite and the Ti Alloy Matrix," NASA Report TM-101984, National Aeronautics and Space Administration, Lewis Research Center, Cleveland, OH, Apr. 1989.

5. Gabb, T.P., Gayda, J.G., and MacKay, R.A., "Isothermal and Nonisothermal Fatigue Behavior of a Metal Matrix Composite," Submitted to Journal of Composite Materials.

6. Majumdar, B.S., and Newaz, G.M., "Thermo-Mechanical Fatigue of an Angle-Ply Metal Matrix Composite," Presented at ASTM Third Symposium on Composite Materials: Fatigue and Fracture, Orlando, FL, Nov. 1989.

7. Bania, P.J., Lenning, G.A., and Hall, J.A., in Beta Titanium Alloys in the 80's, R.R Boyer and H.W. Rosenberg, Eds., TMS-AIME, Warrendale, PA, 1984, pp. 209-230.

8. Duerig, T.W., and Williams, J.C., in Beta Titanium Alloys in the 80's, R.R Boyer and H.W. Rosenberg, Eds., TMS-AIME, Warrendale, PA, 1984, pp. 19-67.

9. Lerch, B.A., Gabb, T.P., and MacKay, R.A., "Heat Treatment Study of the SiC/Ti-15-3 Composite System," NASA Report TP-2970, National Aeronautics and Space Administration, Lewis Research Center, Cleveland, OH, Jan. 1990.

10. Ellis, J.R., and Bartolotta, P.A., "A Fixture Facilitating the Use of Induction Heating in Mechanical Testing," NASA Report TM-102416, National Aeronautics and Space Administration, Lewis Research Center, Cleveland, OH, June 1990.

11. Rosenberg, H.W., in Beta Titanium Alloys in the 80's, R.R Boyer and H.W. Rosenberg, Eds., TMS-AIME, Warrendale, PA, 1984, pp. 409-432.

12. Castelli, M.G., Bartolotta, P.A., Ellis, R., Ervin, D.R., and Heine, J.E., in HITEMP Review 1989: Advanced High Temperature Engine Materials Technology Program, NASA Report CP-10039, National Aeronautics and Space Administration, Lewis Research Center, Cleveland, OH, Oct. 1989, pp. 43:1-43:14.

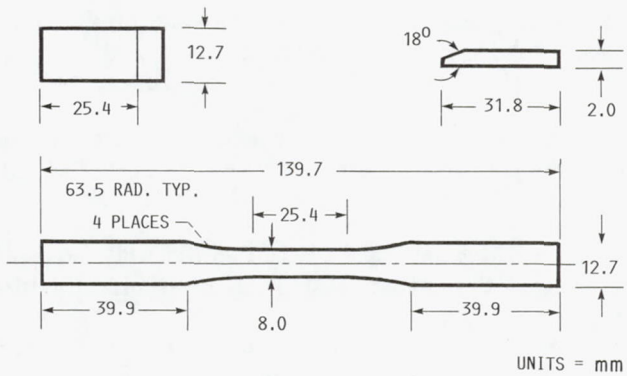

FIGURE 1. - TEST SPECIMEN GEOMETRY AND TAB DETAILS.

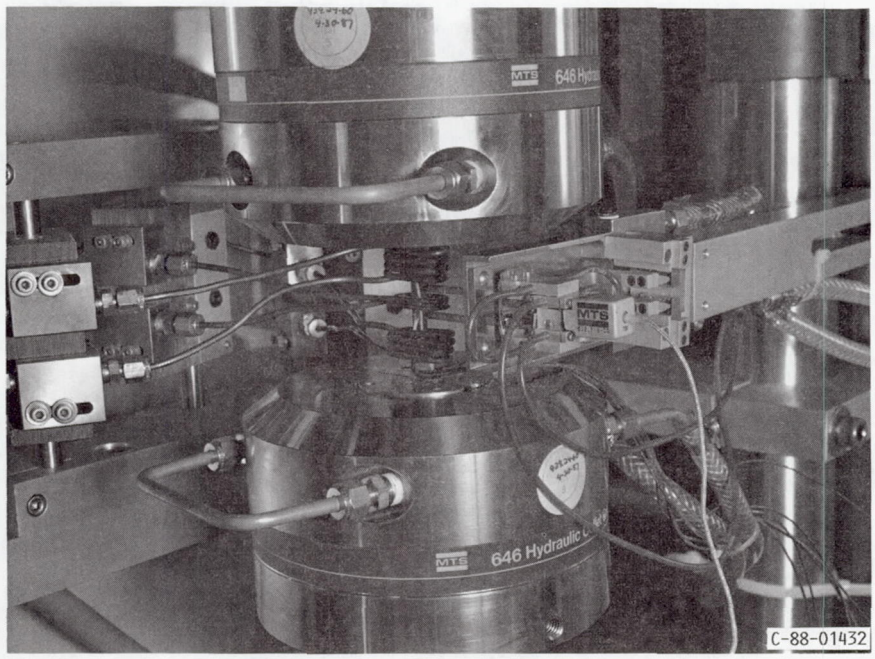

FIGURE 2. - SERVO-HYDRAULIC LOAD TRAIN.

	MAXIMUM STRESS, MPa				
	1241	1034	965	896	827
ISOTHERMAL 427 ^{o}C (FURNACE HEATING)		1	1	1	
TMF OUT-OF-PHASE 93 ^{o}C - 538 ^{o}C (DIRECT INDUCTION HEATING)	2	2		2	2
TMF IN-PHASE 93 ^{o}C - 538 ^{o}C (DIRECT INDUCTION HEATING)		2	2	2	2

ALL TESTS WERE PERFORMED UNDER TENSION-TENSION CONDITIONS WITH A STRESS RATIO R_{σ} = 0.05.

FIGURE 3. - TEST MATRIX.

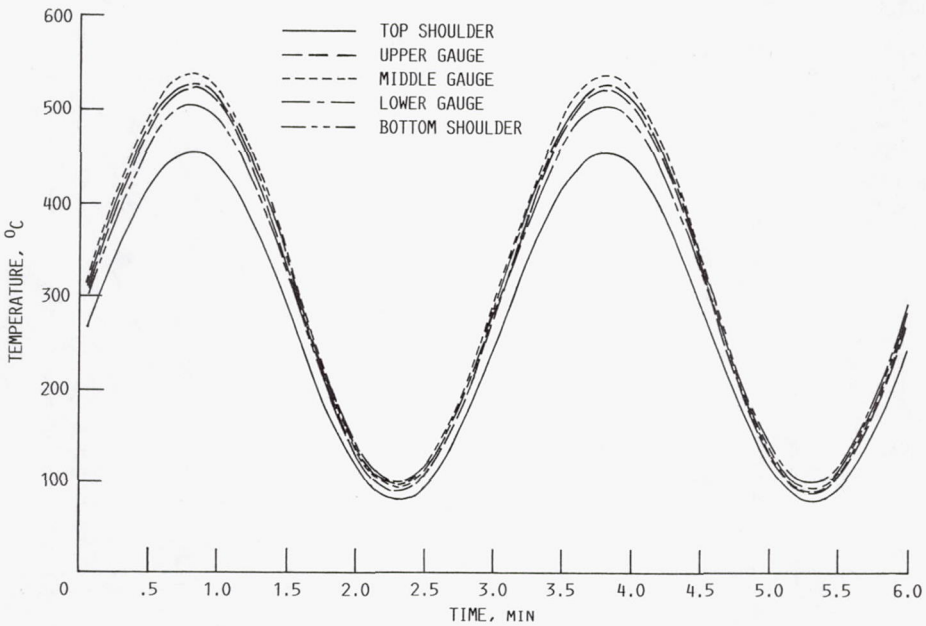

FIGURE 4. - DYNAMIC LONGITUDINAL TEMPERATURE PROFILE.

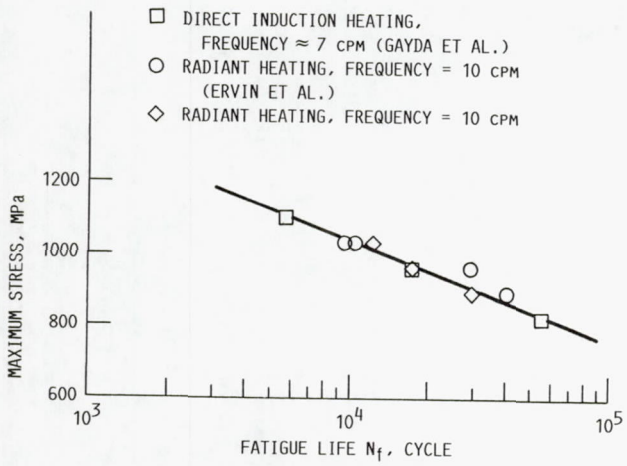

FIGURE 5. - COMPARISON OF ISOTHERMAL FATIGUE LIFE OF SiC/Ti-15-3, $[0]_8$, AT 427 ^{o}C.

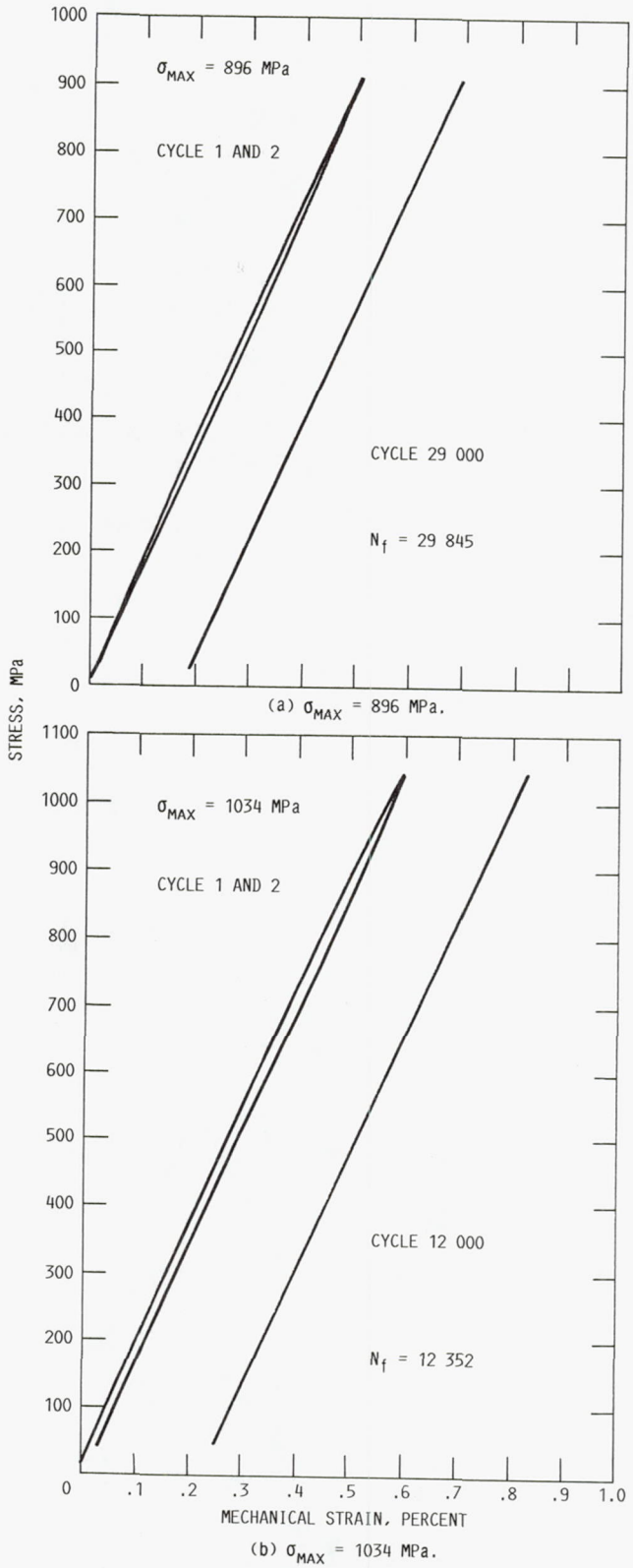

FIGURE 6. - STRESS-STRAIN RESPONSE FOR TWO ISOTHERMAL FATIGUE TESTS AT 427 ^{o}C.

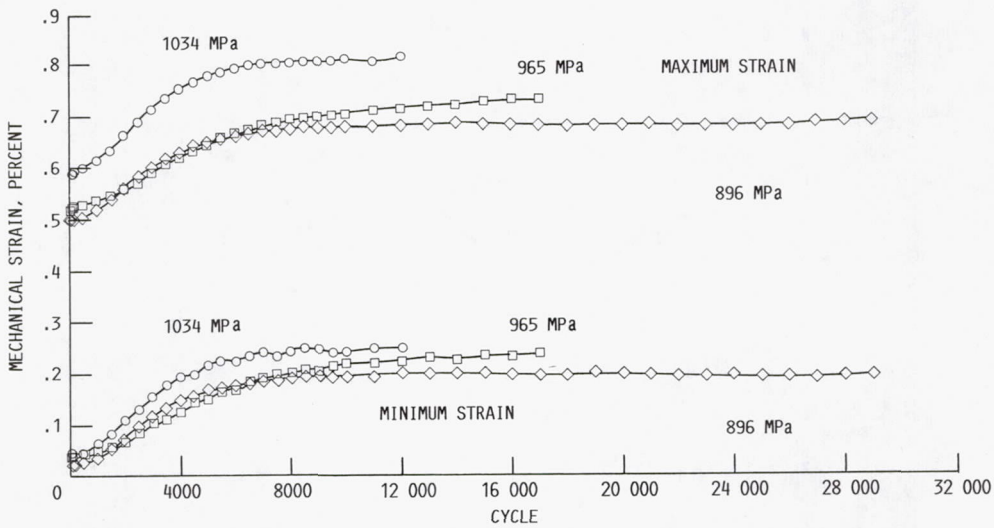

FIGURE 7. - CHANGE IN MAXIMUM AND MINIMUM STRAIN DURING ISOTHERMAL FATIGUE TESTS PERFORMED AT 427 ^{o}C.

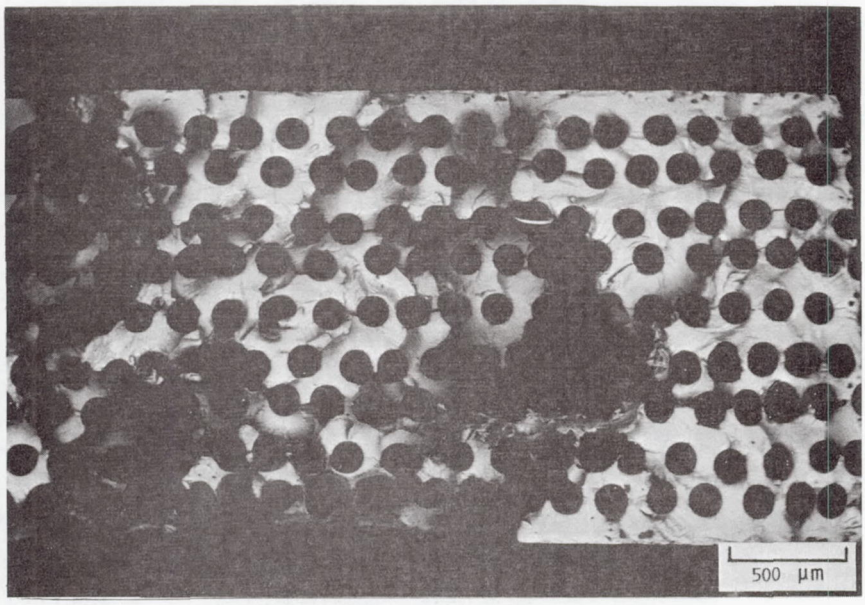

(a) 30X.

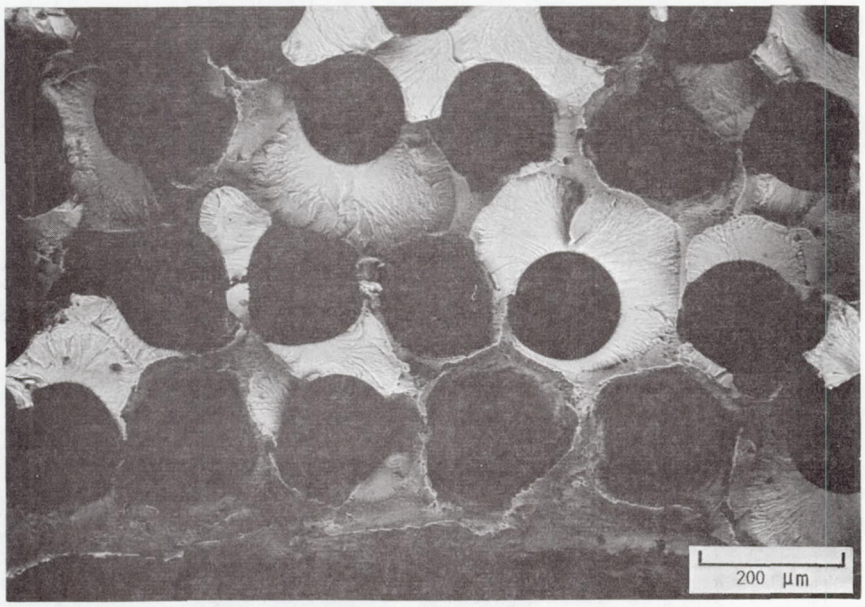

(b) 100X.

FIGURE 8. - TYPICAL SEM BACKSCATTER FRACTORGRAPHS TAKEN FROM THE σ_{MAX} = 896 MPa ISO-THERMAL TEST PERFORMED AT 427 ^{o}C.

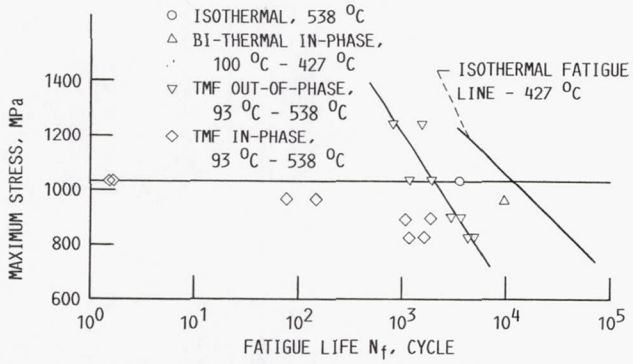

FIGURE 9. - THERMOMECHANICAL FATIGUE LIFE RESULTS FOR SiC/Ti-15-3, $[0]_9$.

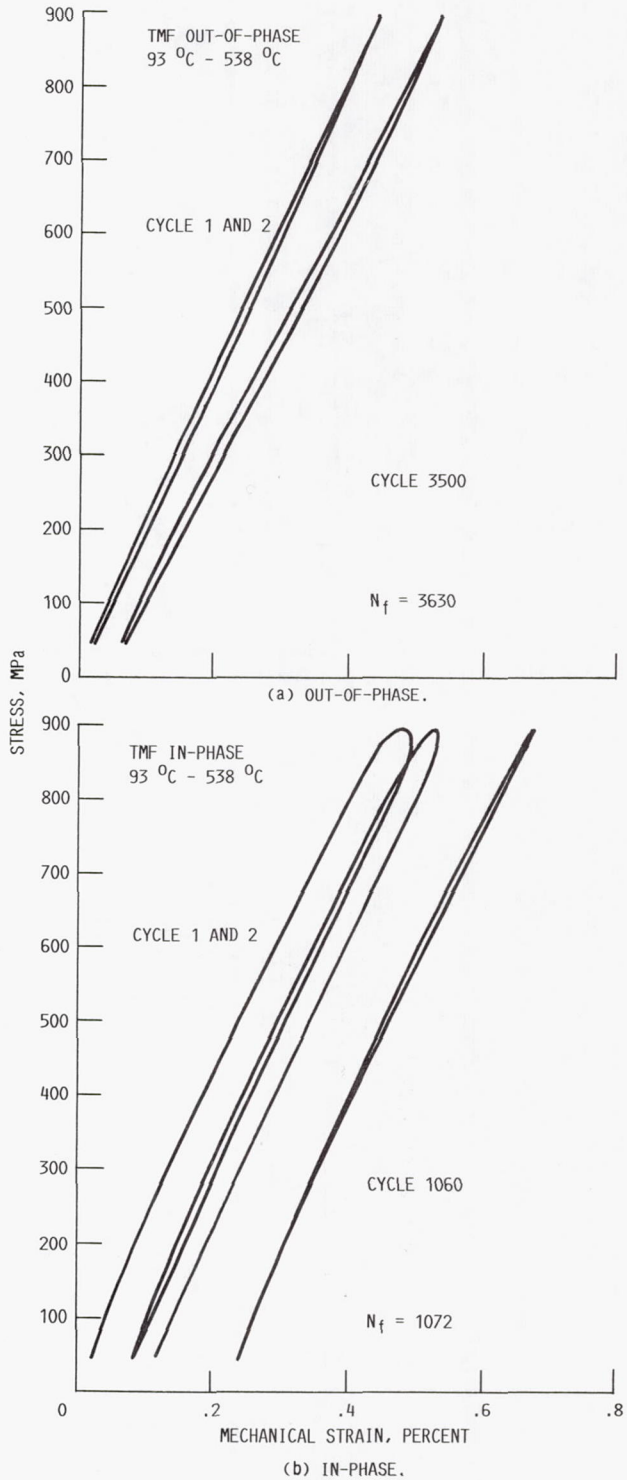

FIGURE 10. - STRESS-MECHANICAL STRAIN RESPONSE FOR TWO THERMOMECHANICAL TESTS PERFORMED AT σ_{MAX} = 896 MPa.

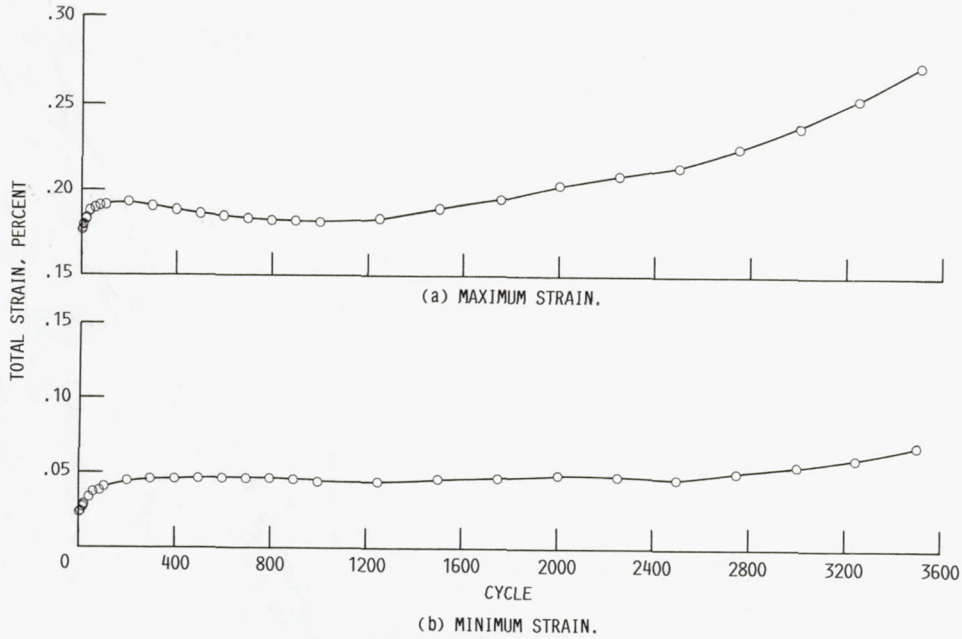

FIGURE 11. - CHANGE IN MAXIMUM AND MINIMUM STRAIN FOR AN OUT-OF-PHASE TEST WITH σ_{MAX} = 896 MPa.

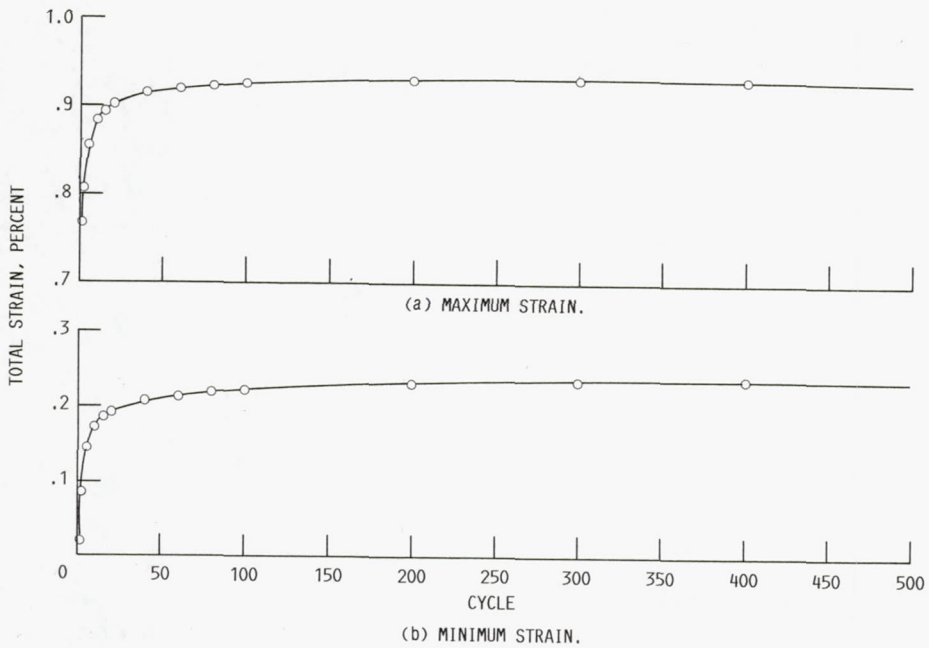

FIGURE 12. - CHANGE IN MAXIMUM AND MINIMUM STRAIN FOR AN IN-PHASE TEST WITH σ_{MAX} = 896 MPa.

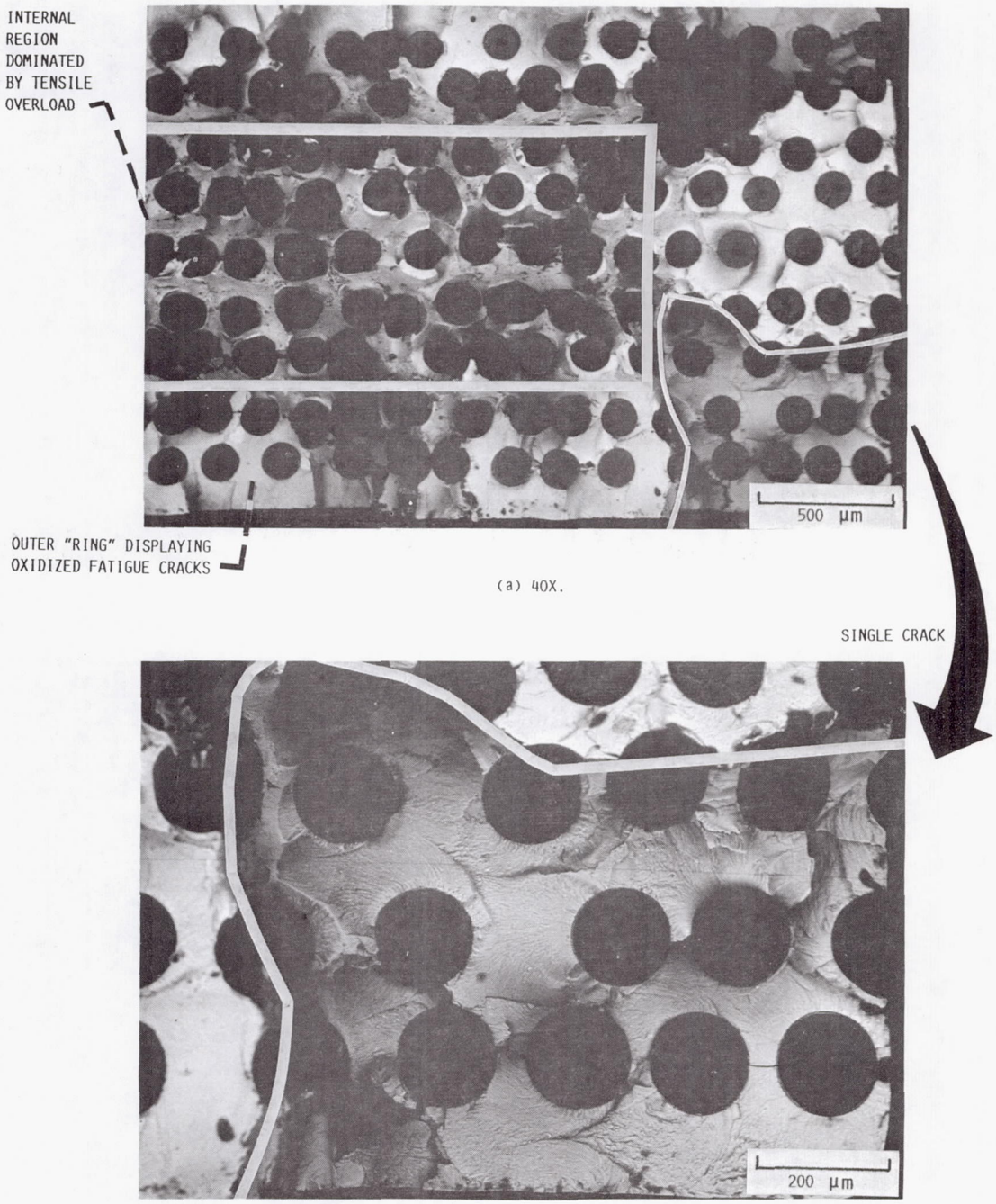

(a) 40X.

(b) 100X.

FIGURE 13. - TYPICAL SEM BACKSCATTER FRACTORGRAPHS TAKEN FROM A SPECIMEN SUBJECTED TO OUT-OF-PHASE LOADING WITH σ_{MAX} = 896 MPa.

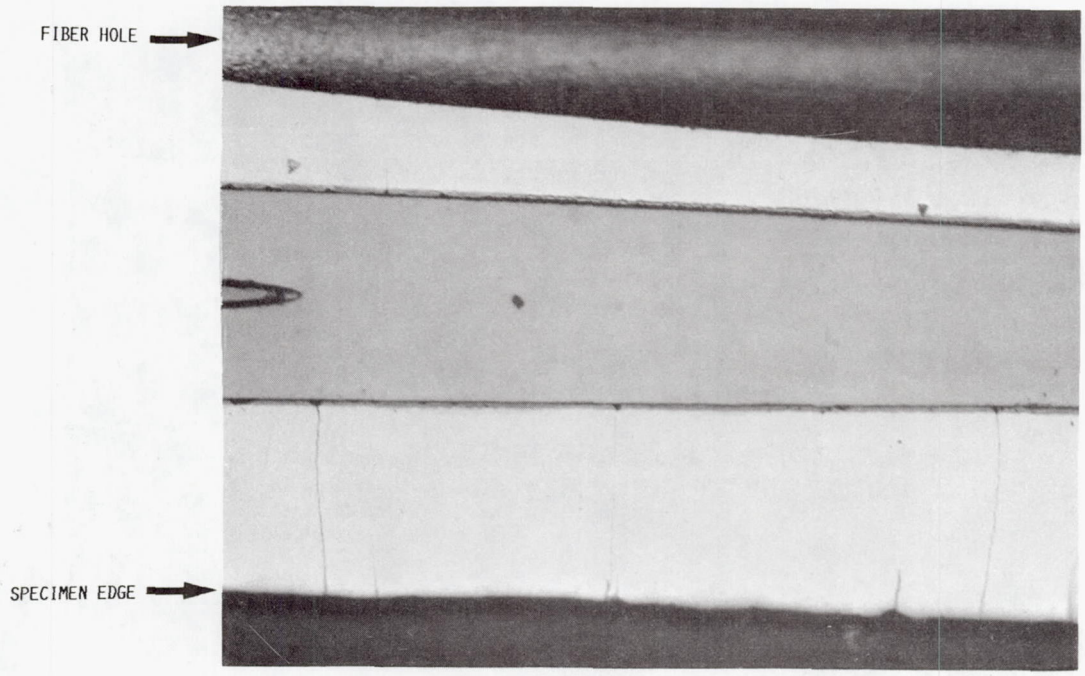

(a) LONGITUDINAL.

100 μM

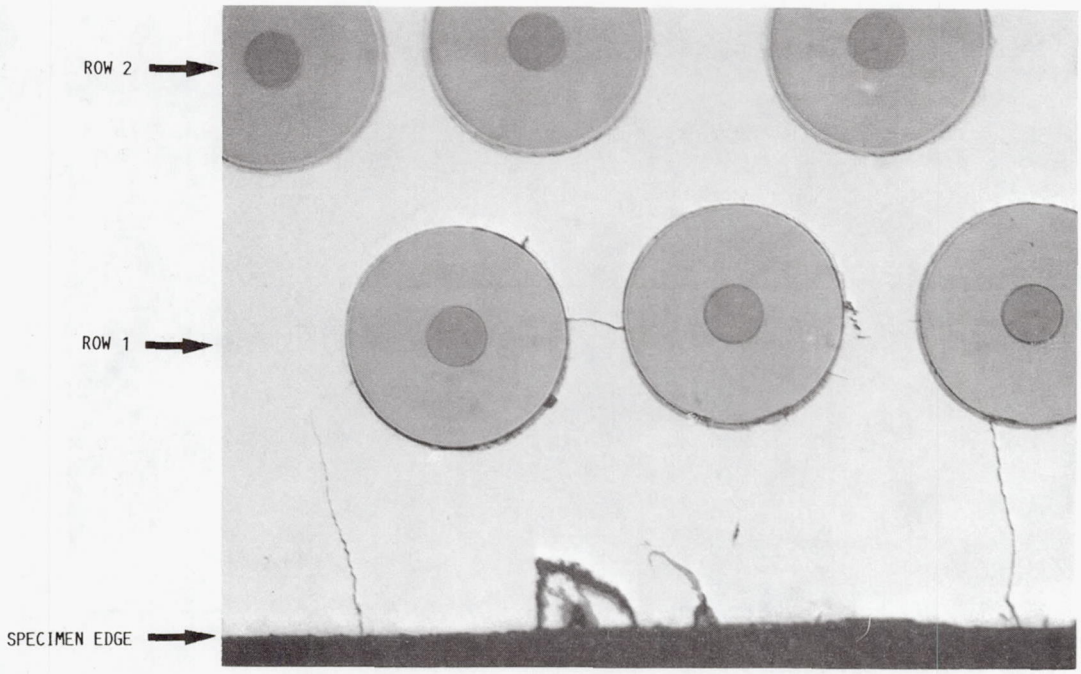

(b) TRANSVERSE.

100 μM

FIGURE 14. - TYPICAL SECTIONS TAKEN FROM A SPECIMEN SUBJECTED TO OUT-OF-PHASE LOADING WITH σ_{MAX} = 896 MPa.

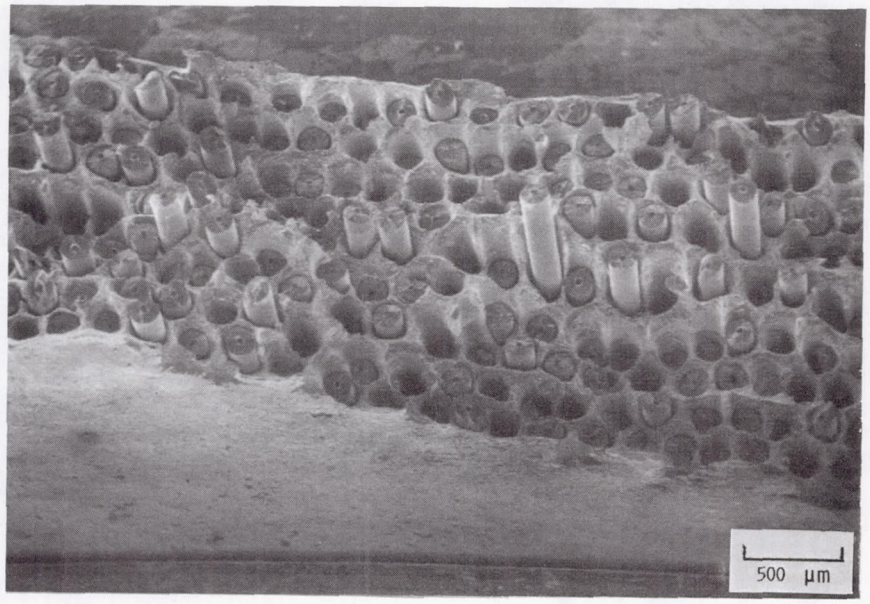

(a) 30X.

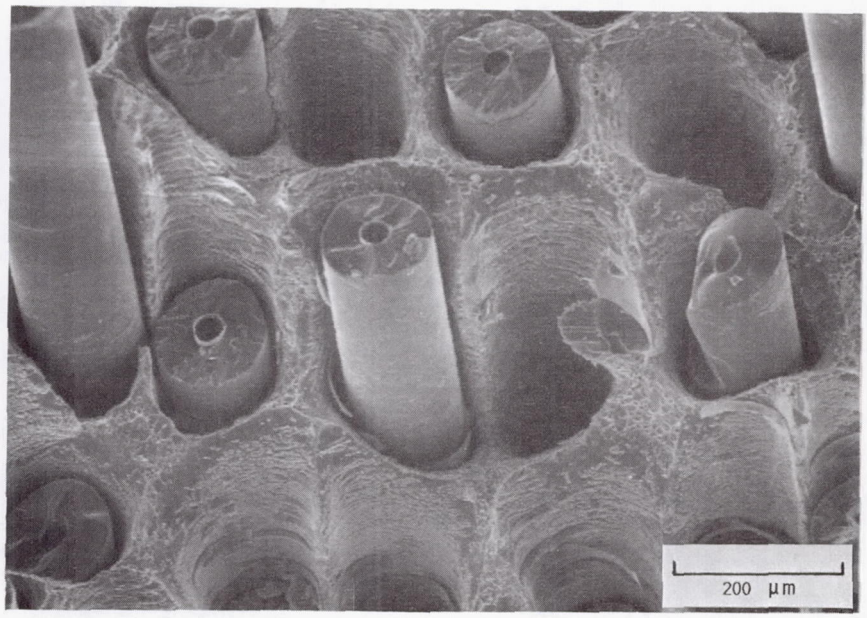

(b) 100X.

FIGURE 15. - TYPICAL SEM FRACTOGRAPHS TAKEN FROM A SPECIMEN SUBJECTED TO IN-PHASE LOADING WITH σ_{MAX} = 896 MPa.

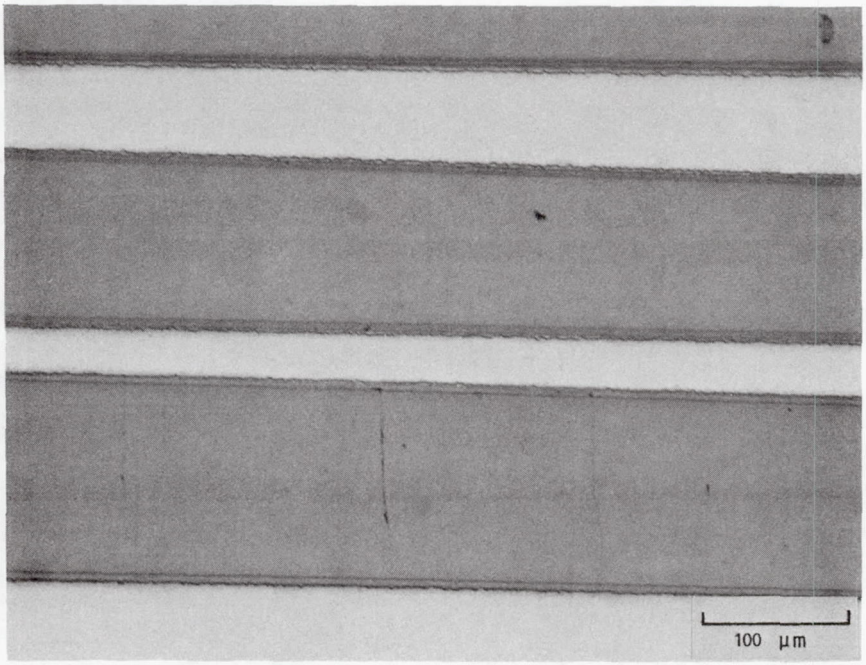

(a) THROUGH THE WIDTH.

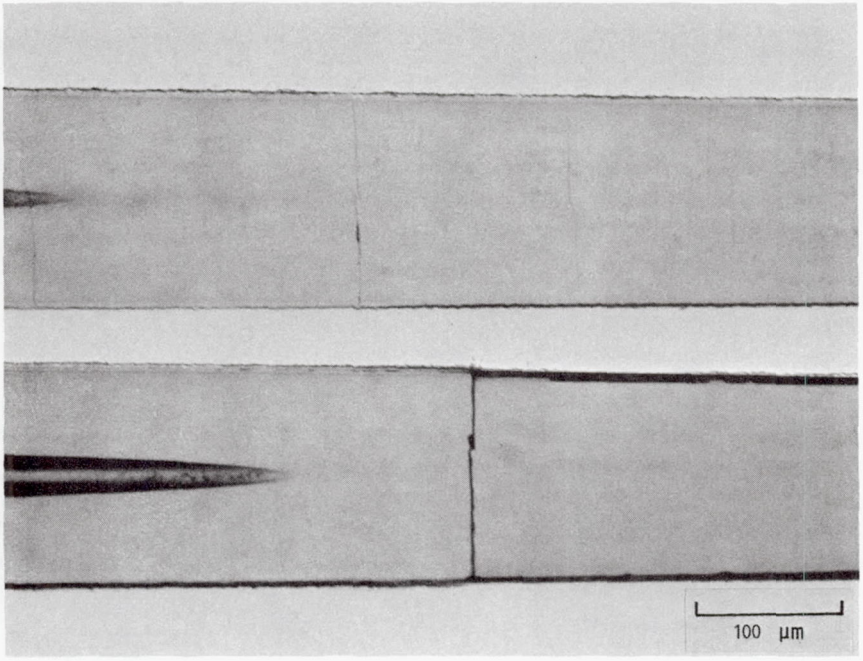

(b) THROUGH THE THICKNESS.

FIGURE 16. - TYPICAL LONGITUDINAL SECTIONS TAKEN FROM A SPECIMEN SUBJECTED TO IN-PHASE LOADING WITH σ_{MAX} = 896 MPa.

NASA
National Aeronautics and Space Administration

Report Documentation Page

1. Report No.	2. Government Accession No.	3. Recipient's Catalog No.
NASA TM-103171		

4. Title and Subtitle

Thermomechanical Testing Techniques for High-Temperature Composites: TMF Behavior of SiC(SCS-6)/Ti-15-3

5. Report Date

6. Performing Organization Code

7. Author(s)

Michael G. Castelli, J. Rodney Ellis, and Paul A. Bartolotta

8. Performing Organization Report No.

E-5543

10. Work Unit No.

505-63-1B

9. Performing Organization Name and Address

National Aeronautics and Space Administration
Lewis Research Center
Cleveland, Ohio 44135-3191

11. Contract or Grant No.

13. Type of Report and Period Covered

Technical Memorandum

12. Sponsoring Agency Name and Address

National Aeronautics and Space Administration
Washington, D.C. 20546-0001

14. Sponsoring Agency Code

15. Supplementary Notes

Prepared for the 10th Symposium on Composite Materials: Testing and Design sponsored by the American Society for Testing and Materials, San Francisco, California, August 24-25, 1990. Michael G. Castelli, Sverdrup Technology, Inc., Lewis Research Center Group, 2001 Aerospace Parkway, Brook Park, Ohio 44142. J. Rodney Ellis and Paul A. Bartolotta, NASA Lewis Research Center.

16. Abstract

Thermomechanical testing techniques recently developed for monolithic structural alloys were successfully extended to continuous fiber reinforced composite materials in plate form. The success of this adaptation was verified on a model metal matrix composite (MMC) material, namely SiC(SCS-6)/Ti-15V-3Cr-3Al-3Sn. Effects of heating system type and specimen preparation are also adressed. Cyclic lives determined under full thermomechanical conditions were shown to be significantly reduced from those obtained under comparable isothermal and in-phase bi-thermal conditions. Fractography and metallography from specimens subjected to isothermal, out-of-phase and in-phase conditions reveal distinct differences in damage/failure modes. Isothermal metallography revealed extensive matrix cracking associated with fiber damage throughout the entire cross-section of the specimen. Out-of-phase metallography revealed extensive matrix damage associated with minimal (if any) fiber cracking. However, the damage was located exculsively at surface and near-surface locations. In-phase conditions produced extensive fiber cracking throughout the entire cross-section, associated with minimal (if any) matrix damage.

17. Key Words (Suggested by Author(s))	18. Distribution Statement
Thermomechanical fatigue Metal matrix composites SiC/Ti-15-3 Damage/failure mode	Unclassified – Unlimited Subject Category 39

19. Security Classif. (of this report)	20. Security Classif. (of this page)	21. No. of pages	22. Price*
Unclassified	Unclassified	20	A03

NASA FORM 1626 OCT 86

*For sale by the National Technical Information Service, Springfield, Virginia 22161